DAFTAR PUSTAKA

Alsharif, S. A., Badran, M. I., Moustafa, M. H., Meshref, R. A., & Mohamed, E. I. (2023). Hydrothermal extraction and physicochemical characterization of biogenic hydroxyapatite nanoparticles from buffalo waste bones for in vivo xenograft in experimental rats. *Scientific Reports*, *13*(1), 1–13. https://doi.org/10.1038/s41598-023-43989-9

Bouropoulos, N., Stampolakis, A., & Mouzakis, D. E. (2010). Dynamic mechanical properties of calcium alginate-hydroxyapatite nanocomposite hydrogels. *Science of Advanced Materials*, *2*(2), 239–242. https://doi.org/10.1166/sam.2010.1092

Cerqueni, G., Scalzone, A., Licini, C., Gentile, P., & Mattioli-Belmonte, M. (2021). Insights into oxidative stress in bone tissue and novel challenges for biomaterials. *Materials Science and Engineering C*, *130*(June), 112433. https://doi.org/10.1016/j.msec.2021.112433

Chandrasekar, A., Sagadevan, S., & Dakshnamoorthy, A. (2013). Synthesis and characterization of nano-hydroxyapatite (n-HAP) using the wet chemical technique. *International Journal of Physical Sciences*, *8*(32), 1639–1645. https://doi.org/10.5897/IJPS2013.3990

Firdaus Hussin, M. S., Abdullah, H. Z., Idris, M. I., & Abdul Wahap, M. A. (2022). Extraction of natural hydroxyapatite for biomedical applications—A review. *Heliyon*, *8*(8), e10356. https://doi.org/10.1016/j.heliyon.2022.e10356

Gheisari, H., Karamian, E., & Abdellahi, M. (2015). A novel hydroxyapatite - Hardystonite nanocomposite ceramic. *Ceramics International*, *41*(4), 5967–5975. https://doi.org/10.1016/j.ceramint.2015.01.033

Hajar Saharudin, S., Haslinda Shariffuddin, J., Ida Amalina Ahamad Nordin, N., & Ismail, A. (2019). Effect of Aging Time in the Synthesis of Biogenic Hydroxyapatite Derived from Cockle Shell. *Materials Today: Proceedings*, *19*, 1208–1215. https://doi.org/10.1016/j.matpr.2019.11.124

Hossain, M. S., Uddin, M. N., Sarkar, S., & Ahmed, S. (2022). Crystallographic dependency of waste cow bone, hydroxyapatite, and β-tricalcium phosphate for biomedical application. *Journal of Saudi Chemical Society*, *26*(6), 101559. https://doi.org/10.1016/j.jscs.2022.101559

Kesmez, Ö. (2020). Preparation of anti-bacterial biocomposite nanofibers fabricated by electrospinning method. *Journal of the Turkish Chemical Society, Section A: Chemistry*, *7*(1), 125–142. https://doi.org/10.18596/jotcsa.590621

Li, J., Deng, C., Liang, W., Kang, F., Bai, Y., Ma, B., Wu, C., & Dong, S. (2021). Mn-containing bioceramics inhibit osteoclastogenesis and promote osteoporotic bone regeneration via scavenging ROS. *Bioactive Materials*, *6*(11), 3839–3850. https://doi.org/10.1016/j.bioactmat.2021.03.039

Li, Y., Liu, Y., Li, R., Bai, H., Zhu, Z., Zhu, L., Zhu, C., Che, Z., Liu, H., Wang, J., & Huang, L. (2021). Collagen-based biomaterials for bone tissue engineering. *and Design*, *210*, 110049. 0.1016/j.matdes.2021.110049

i, B., Rahimiopour, M. R., Sadrnezhaad, S. K., Amin, M. H., & (2008). Synthesis of nano-hydroxyapatite under a ydrothermal condition. *Biomedical Materials*, *3*(2). 0.1088/1748-6041/3/2/025002

aj, D., Ponpandian, N., & Viswanathan, C. (2015). Core-shell Mg nanostructures: Surfactant free facile synthesis, characterization and their in vitro cell viability studies against leukaemia cancer cells (K562). *RSC Advances*, *5*(60), 48705–48711. https://doi.org/10.1039/c5ra04663g

Mocanu, A. C., Stan, G. E., Maidaniuc, A., Miculescu, M., Antoniac, I. V., Ciocoiu, R. C., Voicu, Ş. I., Mitran, V., Cîmpean, A., & Miculescu, F. (2019). Naturally-derived biphasic calcium phosphates through increased phosphorus-based reagent amounts for biomedical applications. *Materials*, *12*(3), 1–17. https://doi.org/10.3390/ma12030381

Ou, K. L., Hou, P. J., Huang, B. H., Chou, H. H., Yang, T. Sen, Huang, C. F., & Ueno, T. (2020). Bone healing and regeneration potential in rabbit cortical defects using an innovative bioceramic bone graft substitute. *Applied Sciences (Switzerland)*, *10*(18). https://doi.org/10.3390/APP10186239

Permatasari, H. A., & Yusuf, Y. (2019). Characteristics of Carbonated Hydroxyapatite Based on Abalone Mussel Shells (Halioitis asinina) Synthesized by Precipitation Method with Aging Time Variations. *IOP Conference Series: Materials Science and Engineering*, *546*(4). https://doi.org/10.1088/1757-899X/546/4/042031

Pourmollaabbassi, B., Karbasi, S., & Hashemibeni, B. (2016). Evaluate the growth and adhesion of osteoblast cells on nanocomposite scaffold of hydroxyapatite/titania coated with poly hydroxybutyrate. *Advanced Biomedical Research*, *5*(1), 156. https://doi.org/10.4103/2277-9175.188486

Prawira, S. E., Triyono, J., Triyono, T., & Graft, B. (2019). *PENGARUH TEMPERATUR KALSINASI TERHADAP SIFAT MEKANIK Mekanika : Majalah Ilmiah Mekanika 23*. *18*, 22–27.

Sahana, H., Khajuria, D. K., Razdan, R., Mahapatra, D. R., Bhat, M. R., Suresh, S., Rao, R. R., & Mariappan, L. (2013). Improvement in bone properties by using risedronate adsorbed hydroxyapatite novel nanoparticle based formulation in a rat model of osteoporosis. *Journal of Biomedical Nanotechnology*, *9*(2), 193–201. https://doi.org/10.1166/jbn.2013.1482

Sari, M., Hening, P., Chotimah, Ana, I. D., & Yusuf, Y. (2021a). Bioceramic hydroxyapatite-based scaffold with a porous structure using honeycomb as a natural polymeric Porogen for bone tissue engineering. *Biomaterials Research*, *25*(1), 1–13. https://doi.org/10.1186/s40824-021-00203-z

Sari, M., Hening, P., Chotimah, Ana, I. D., & Yusuf, Y. (2021b). Porous structure of bioceramics carbonated hydroxyapatite-based honeycomb scaffold for bone tissue engineering. *Materials Today Communications*, *26*(January), 102135. https://doi.org/10.1016/j.mtcomm.2021.102135

Susanto, R. (2021). Potensi Pembuatan Replika Tulang Berpori Menggunakan Template Ampas Tebu. *Chempublish Journal*, *5*(2), 116–129. https://doi.org/10.22437/chp.v5i2.10612

Tanpure, S., Ghanwat, V., Shinde, B., Tanpure, K., & Lawande, S. (2022). The Eggshell Waste Transformed Green and Efficient Synthesis of K-Ca(OH)2 om Temperature Synthesis of Chalcones. *Polycyclic Aromatic* *42*(4), 1322–1340. 0.1080/10406638.2020.1776740

ng, H. F., & Koleangan, H. S. J. (2020). SINTESIS L Ag/CoFe2O4 MENGGUNAKAN EKSTRAK DAUN nredera cordifolia (Ten) Steenis) DAN APLIKASINYA TOKATALIS UNTUK MENDEGRADASI ZAT WARNA BLUE. *Chemistry Progress*, *12*(2), 59–66.

https://doi.org/10.35799/cp.12.2.2019.27924

Wong, C. C., Yeh, Y. Y., Chen, C. H., Manga, Y. B., Jheng, P. R., Lu, C. X., & Chuang, E. Y. (2021). Effectiveness of treating segmental bone defects with a synergistic co-delivery approach with platelet-rich fibrin and tricalcium phosphate. *Materials Science and Engineering C*, *129*(July), 112364. https://doi.org/10.1016/j.msec.2021.112364

Wu, C. J., Liu, K. F., Liu, C. M., Lan, W. C., Chu, S. F., Shen, Y. K., Huang, B. H., Huang, J., Cho, Y. C., Ou, K. L., & Peng, P. W. (2023). An innovative biomimetic porous bioceramic to facilitate bone tissue regeneration: Microstructural characteristics, biocompatibility, and in vivo rabbit model evaluation. *Journal of Materials Research and Technology*, *22*, 2566–2575. https://doi.org/10.1016/j.jmrt.2022.12.089

Zhang, H., Zhang, H., Xiong, Y., Dong, L., & Li, X. (2021). Development of hierarchical porous bioceramic scaffolds with controlled micro/nano surface topography for accelerating bone regeneration. *Materials Science and Engineering C*, *130*(July), 112437. https://doi.org/10.1016/j.msec.2021.112437

Zhao, R., Shang, T., Yuan, B., Zhu, X., Zhang, X., & Yang, X. (2022). Osteoporotic bone recovery by a bamboo-structured bioceramic with controlled release of hydroxyapatite nanoparticles. *Bioactive Materials*, *17*(January), 379–393. https://doi.org/10.1016/j.bioactmat.2022.01.007

Zhi, W., Wang, X., Sun, D., Chen, T., Yuan, B., Li, X., Chen, X., Wang, J., Xie, Z., Zhu, X., Zhang, K., & Zhang, X. (2022). Optimal regenerative repair of large segmental bone defect in a goat model with osteoinductive calcium phosphate bioceramic implants. *Bioactive Materials*, *11*(June 2021), 240–253. https://doi.org/10.1016/j.bioactmat.2021.09.024

LAMPIRAN

Lampiran 1. Dokumentasi Penelitian

1. Pembuatan Serbuk CaO

Tulang Kerbau

Tulang kerbau di keringkan dibawah sinar matahari

Tulang kerbau dihancurkan menjadi serpihan kecil

Tulang kerbau diblender

u diayak

Kalsinasi tulang kerbau

Serbuk CaO

2. Pembuatan Serbuk HAp

Serbuk Kalsium oksida (CaO)

Serbuk Diamonium hidrogen fosfat ($(NH_4)_2HPO_4$)

tan CaO

Larutan ($(NH_4)_2HPO_4$)

Pencampuran larutan $((NH_4)_2HPO_4)$ ke dalam larutan CaO

Proses pengendapan

Proses Penyaringan

Hasil penyaringan

ven

Proses sintering HAp

Serbuk Hidroksiapatit

3. Pembuatan *Scaffold* HA


Serbuk HAp


Madu

Pencampuran madu
ke dalam larutan HAp


Sampel di oven

Scaffold 20% HCB

Scaffold 40% HCB

Scaffold 60% HCCB

Lampiran 2. Analisi Data FTIR

1. Data FTIR untuk sampel tanpa HCB

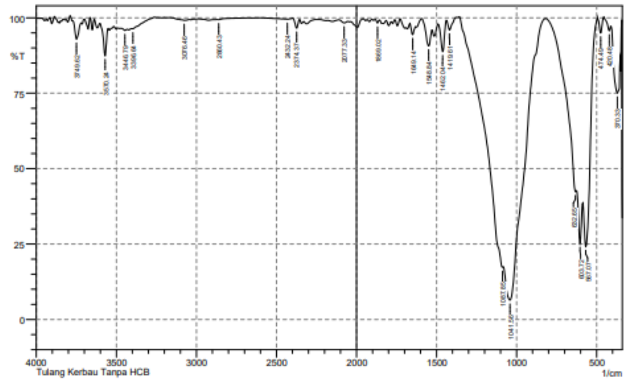

No.	Peak	Intensity	Corr. Intensity	Base (H)	Base (L)	Area	Corr. Area
1	370.33	75.084	5.251	408.91	360.69	4.363	1.11
2	420.48	95.671	2.189	455.2	410.84	0.413	0.165
3	474.49	94.994	5.18	493.78	455.2	0.397	0.426
4	567.07	24.193	27.384	586.36	495.71	25.378	8.635
5	603.72	25.222	14.953	624.94	588.29	17.82	3.373
6	632.65	42.346	2.062	817.82	626.87	21.495	0.139
7	1041.56	6.449	23.686	1082.07	819.75	110.101	25.958
8	1087.85	17.311	1.324	1355.96	1083.99	66.93	0.189
9	1419.61	95.975	3.496	1438.9	1377.17	0.514	0.42
10	1462.04	88.77	9.839	1490.97	1438.9	1.398	1.07
11	1548.84	90.687	6.421	1591.27	1529.55	1.491	0.878
12	1649.14	94.443	3.134	1666.5	1631.78	0.624	0.254
13	1869.02	98.264	1.071	1884.45	1857.45	0.13	0.054
14	2077.33	98.289	0.727	2108.2	2056.12	0.3	0.088
15	2374.37	96.587	3.048	2399.45	2357.01	0.325	0.265
16	2432.24	99.519	0.399	2601.97	2399.45	0.209	0.165
17	2860.43	99.397	0.044	2872.01	2675.27	0.177	-0.089
18	3076.46	99.147	0.455	3165.19	3045.6	0.248	0.119
19	3396.64	96.368	0.192	3402.43	3265.49	0.997	0.024
20	3446.79	95.803	0.474	3469.94	3433.29	0.628	0.031
21	3570.24	87.481	9.504	3603.03	3552.88	1.506	0.891
22	3749.62	92.924	6.369	3788.19	3720.69	0.984	0.814

2. Data FTIR untuk sampel 20% HCB

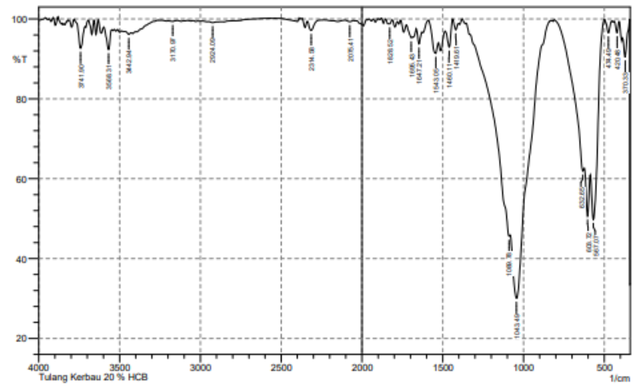

No.	Peak	Intensity	Corr. Intensity	Base (H)	Base (L)	Area	Corr. Area
1	370.33	90.505	6.086	385.76	345.26	1.043	0.528
2	420.48	96.537	2.87	439.77	406.98	0.267	0.184
3	474.49	96.522	3.171	499.56	453.27	0.347	0.289
[illegible]	[illegible]7	49.795	19.833	586.36	499.56	13.101	4.469
[illegible]	[illegible]2	50.637	10.943	623.01	588.29	8.743	1.444
[illegible]	[illegible]5	61.887	2.311	808.17	624.94	13.536	0.182
[illegible]	[illegible].49	30.055	24.012	1082.07	829.39	51.045	12.438
[illegible]	[illegible].78	45.597	1.451	1330.88	1083.99	32.323	0.105
[illegible]	[illegible].61	97.261	2.142	1438.9	1402.25	0.259	0.168
[illegible]	[illegible].11	92.947	5.65	1485.19	1438.9	0.879	0.567
[illegible]	[illegible].05	91.382	4.135	1587.42	1527.62	1.497	0.64
[illegible]	[illegible].21	93.744	3.389	1664.57	1627.92	0.728	0.261
[illegible]	[illegible].43	95.266	0.947	1726.29	1685.79	0.62	0.083
[illegible]	[illegible].52	98.753	0.237	1832.38	1813.09	0.071	0.012
[illegible]	[illegible].41	99.329	0.316	2104.34	2052.26	0.117	0.038
[illegible]	[illegible].58	97.109	2.407	2337.72	2256.71	0.483	0.334
[illegible]	[illegible].09	99.075	0.244	2949.16	2870.08	0.268	0.032
[illegible]	[illegible].97	99.384	0.185	3199.91	3142.04	0.13	0.021
[illegible]	[illegible].94	96.143	0.518	3466.08	3429.43	0.569	0.037
[illegible]	[illegible].31	92.299	5.278	3597.24	3549.02	1.049	0.546
[illegible]	[illegible]9	92.688	6.087	3778.55	3714.9	1.051	0.74

3. Data FTIR untuk sampel 40% HCB

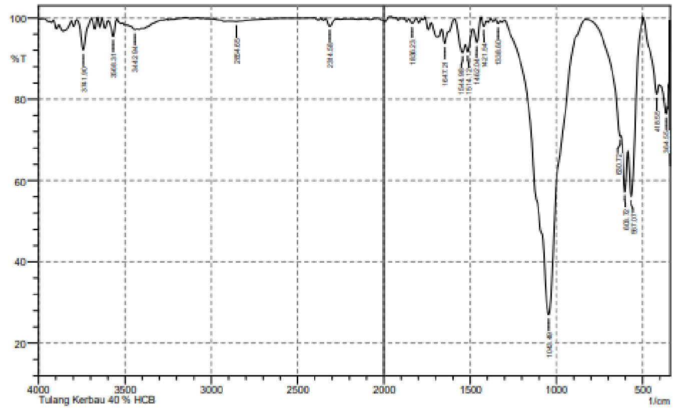

No.	Peak	Intensity	Corr. Intensity	Base (H)	Base (L)	Area	Corr. Area
1	364.55	76.446	1.974	403.12	358.76	4.228	0.129
2	418.55	81.255	4.727	497.63	405.05	4.338	0.698
3	567.07	56.119	17.526	584.43	499.56	10.243	3.404
4	603.72	57.303	11.493	624.94	586.36	7.672	1.422
5	630.72	70.89	0.638	821.68	626.87	8.173	-6.491
6	1043.49	27.004	72.595	1300.02	831.32	71.683	70.839
7	1338.6	98.621	0.819	1354.03	1325.1	0.12	0.051
8	1421.54	97.929	1.78	1436.97	1406.11	0.171	0.132
9	1462.04	94.001	4.703	1485.19	1436.97	0.734	0.471
10	1514.12	91.687	2.958	1527.62	1485.19	1.138	0.277
11	1544.98	91.482	3.554	1589.34	1529.55	1.455	0.521
12	1647.21	93.747	4.028	1664.57	1591.27	1.071	0.594
13	1836.23	98.682	1.235	1855.52	1813.09	0.14	0.126
14	2314.58	97.984	1.908	2337.72	2270.22	0.293	0.251
15	2854.65	99.118	0.119	2902.87	2831.5	0.254	0.015
16	3442.94	97.095	0.392	3489.23	3431.36	0.588	0.023
17	3568.31	95.466	4.064	3597.24	3545.16	0.518	0.406
18	3741.9	92.077	7.609	3778.55	3697.54	1.267	1.164

4.Data FTIR untuk sampel 60% HCB

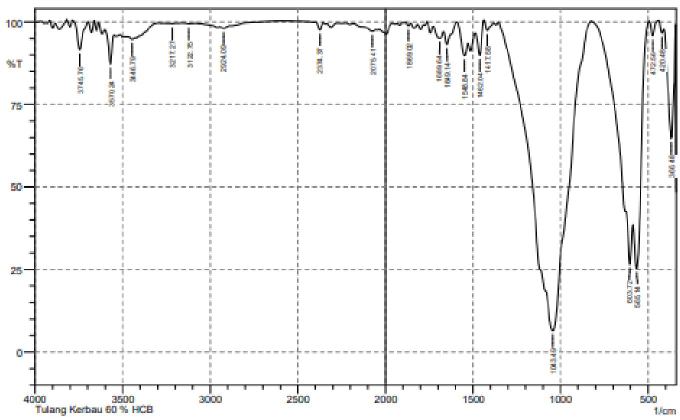

No.	Peak	Intensity	Corr. Intensity	Base (H)	Base (L)	Area	Corr. Area
1	366.48	64.907	30.762	408.91	345.26	6.636	5.538
2	420.48	96.634	2	439.77	410.84	0.241	0.123
3	472.56	95.824	4.457	495.71	439.77	0.346	0.419
[illegible]	[illegible]	25.327	26.182	584.43	495.71	24.273	7.817
[illegible]	[illegible]	26.661	13.464	626.87	586.36	19.107	3.11
[illegible]	[illegible]	6.478	93.554	1352.1	823.6	171.14	171.145
[illegible]	[illegible]	97.4	2.832	1436.97	1381.03	0.304	0.328
[illegible]	[illegible]	89.848	8.598	1485.19	1436.97	1.208	0.91
[illegible]	[illegible]	89.708	5.696	1593.2	1529.55	1.715	0.755
[illegible]	[illegible]	93.164	4.563	1666.5	1595.13	1.17	0.701
[illegible]	[illegible]	95.14	2.451	1726.29	1668.43	0.994	0.429
[illegible]	[illegible]	98.799	0.911	1884.45	1855.52	0.09	0.055
[illegible]	[illegible]	97.175	0.7	2183.42	2056.12	0.978	0.154
[illegible]	[illegible]	97.563	2.336	2399.45	2355.08	0.222	0.205
[illegible]	[illegible]	98.042	0.516	2943.37	2883.58	0.414	0.054
[illegible]	[illegible]	99.426	0.147	3143.97	3105.39	0.082	0.012
[illegible]	[illegible]	99.496	0.095	3234.62	3190.26	0.085	0.007
[illegible]	[illegible]	94.773	0.556	3469.94	3431.36	0.84	0.045
[illegible]	[illegible]	87.308	9.331	3601.1	3549.02	1.696	0.95
[illegible]	[illegible]	91.645	8.594	3784.34	3699.47	1.249	1.328

Lampiran 3. Analisis Data XRD

Tabel 1. Analisis Data XRD untuk Ukuran Kristal menggunakan Excel

Sampel	2θ	θ	Cos θ	β	D	Rata-rata D
Tanpa HCB	31.51	15.755	0.9624315	0.21040	40.9755503	41.26662712
	32.65	16.325	0.9596827	0.22160	39.01601782	
	31.93	15.965	0.9614299	0.19700	43.80831324	
20% HCB	31.41	15.705	0.9626681	0.32530	26.49596385	26.05107228
	32.53	16.265	0.9599766	0.35000	24.69515209	
	31.82	15.91	0.9616935	0.32000	26.9621009	
40% HCB	31.93	15.965	0.9614299	0.28470	30.31344471	30.08600848
	33.05	16.525	0.9586957	0.28900	29.94758105	
	32.34	16.17	0.9604396	0.28800	29.99699968	
60% HCB	31.95	15.975	0.9613819	0.85500	10.09434945	14.85315252
	32.95	16.475	0.9589436	0.64330	13.45035594	
	49.63	24.815	0.9076676	0.43500	21.01475217	

Perhitungan ukuran kristal secara manual

$$D = \frac{K\lambda}{\beta \cos \theta}$$

Diketahui: k = 0,94

λ = 0,15406 nm

1. Tanpa HCB
   a. 31,51
      - 2θ = 31,51
        θ = 15,755° → 0,274 radian
      - Cos θ = 0,962
      - β = 0,21040° → 0,00367 radian

❖ D $= \frac{0,94 \times 0,15406}{0,00367 \times 0,962}$

$= \frac{0,1443}{0,00353}$

= 40,88 nm

   b. 32,65

65

325° → 0,285 radian

= 0,958

2160° → 0,00387 radian

406

,958

$= \dfrac{0,1443}{0,00371}$

= 38,89 nm

c. 31,93

- 2θ = 31,93

  θ = 15,965^o → 0,279 radian
- Cos θ = 0,961
- β = 0,19700^o → 0,00344 radian

❖ D $= \dfrac{0,94 \times 0,15406}{0,00344 \times 0,961}$

$= \dfrac{0,1443}{0,00331}$

= 43,59 nm

2. 20% HCB

a. 31,41

- 2θ = 31,41

  θ = 15,705^o → 0,274 radian
- Cos θ = 0,962
- β = 0,32530^o → 0,00567 radian

❖ D $= \dfrac{0,94 \times 0,15406}{0,00567 \times 0,962}$

$= \dfrac{0,1443}{0,00546}$

= 26,43 nm

b. 32,53

- 2θ = 32,53

  θ = 16,265^o → 0,284 radian
- Cos θ = 0,958
- β = 0,35000^o → 0,00611 radian

❖ D $= \dfrac{0,94 \times 0,15406}{0,00611 \times 0,958}$

$= \dfrac{0,1443}{0,00586}$

82

91^o → 0,277 radian

= 0,961

- β = 0,32000° → 0,00559 radian

❖ D $= \dfrac{0,94 \times 0,15406}{0,00559 \times 0,961}$

$= \dfrac{0,1443}{0,00537}$

= 26,87 nm

3. 40% HCB

a. 31,93

- 2θ = 31,93
  θ = 15,965° → 0,278 radian
- Cos θ = 0,961
- β = 0,28470° → 0,00497 radian

❖ D $= \dfrac{0,94 \times 0,15406}{0,00497 \times 0,961}$

$= \dfrac{0,1443}{0,00478}$

= 30,19 nm

b. 33,05

- 2θ = 33,05
  θ = 16,025° → 0,279 radian
- Cos θ = 0,961
- β = 0,28900° → 0,00504 radian

❖ D $= \dfrac{0,94 \times 0,15406}{0,00504 \times 0,961}$

$= \dfrac{0,1443}{0,00484}$

= 29,81 nm

c. 32,34

- 2θ = 32,34
  θ = 16,17° → 0,282 radian
- Cos θ = 0,960
- β = 0,28800° → 0,00503 radian

$\dfrac{0,94 \times 0,15406}{\ldots,960}$

- 2θ = 31,95
  θ = 15,975° → 0,279 radian
- Cos θ = 0,961
- β = 0,85500° → 0,01493 radian

❖ D $= \dfrac{0{,}94 \times 0{,}15406}{0{,}01493 \times 0{,}961}$
$= \dfrac{0{,}1443}{0{,}01435}$
= 10,06 nm

b. 32,95

- 2θ = 32,95
  θ = 16,475° → 0,287 radian
- Cos θ = 0,958
- β = 0,64330° → 0,01123 radian

❖ D $= \dfrac{0{,}94 \times 0{,}15406}{0{,}01123 \times 0{,}958}$
$= \dfrac{0{,}1443}{0{,}01076}$
= 13,41 nm

c. 49,63

- 2θ = 49,63
  θ = 24,815° → 0,433 radian
- Cos θ = 0,904
- β = 0,43500° → 0,00760 radian

❖ D $= \dfrac{0{,}94 \times 0{,}15406}{0{,}00760 \times 0{,}904}$
$= \dfrac{0{,}1443}{0{,}00687}$
= 21,00 nm